Eur Spine J (1998) 7:16–23

ORIGINAL ARTICLE

D. Lemosse
O. Le Rue
A. Diop
W. Skalli
P. Marec
F. Lavaste

Characterization of the mechanical behaviour parameters of the costo-vertebral joint

Received: 13 September 1996
Revised: 25 February 1997
Accepted: 17 March 1997

D. Lemosse · O. Le Rue · A. Diop (✉)
W. Skalli · P. Marec · F. Lavaste
Laboratoire de Biomécanique,
Ecole Nationale Supérieure d'Arts
et Métiers, 151, Boulevard de l'Hôpital,
F-75013 Paris, France
Tel. +33-1-44 24 63 64;
Fax +33-1-44 24 63 66;
e-mail: amadou.diop@paris.ensam.fr

Abstract This in vitro study introduces a new method to determine quantitative parameters characterizing the mechanical behaviour of the costo-vertebral joint. These parameters are useful in building numerical models of the thoracic spine, taking into account the thoracic cage. Nine thoracic cages were isolated from fresh human cadavers. From each cage, three functional units were tested: T1–T2, T5–T6, T9–T10. Loads were applied according to the joint local coordinate system. Every functional unit was tested first intact and again after section of successive costo-transverse ligaments. We used an opto-electronic system to follow the three-dimensional motion of the joint, and obtained non-linear load/displacement curves according to the primary rotation axis. A statistical analysis of these curves allowed the calculation of parameters describing the joint mechanical behaviour: total range of motion, motion in the low-stiffness zone, and flexibilities in the positive and negative quasi-linear zones. These values can be used as a database for mechanical modeling of the spine.

Key words Biomechanics · Costo-vertebral joint · Thoracic spine · Opto-electronic analysis

Introduction

The thoracic cage has an important role in breathing [11] and spine stability, particularly in scoliosis. Thus, knowledge of the costo-vertebral joint behaviour becomes crucial in building a finite-element model of the entire spine including the thoracic cage [2].

At the present time, very little information about costo-vertebral joint behaviour is available in the scientific literature [1, 2, 4, 9]. Furthermore, such information as there is is qualitative rather than quantitative and not useful for mechanical modeling. We aimed to determine the required mechanical data. A preliminary study [3] allowed us to plot some load/displacement curves; however, the measuring systems commonly used by other workers in the field were not suitable for studying such a low-stiffness joint.

The objective of this study is to introduce a new method to analyse the three-dimensional (3D) mechanical behaviour of the costo-vertebral joint using an opto-electronic system.

Materials and methods

Anatomical samples

Nine thoracic cages (Table 1) were isolated from fresh cadavers, at an average of 9 days after death (range 4–11 days). The average age of the subjects was 61 years (range 39–71 years), the average weight was 70 kg (range 46–110 kg) and the average height was 167 cm (range 160–180 cm). There were ten males and one female

Table 1 Anatomical subects (*Delay* time from death to harvesting of specimens)

Subject	0	1	2	3	6	7	8	9	10
Sex	M	M	M	M	F	M	M	M	M
Age (years)	71	62		62	56	59	68	71	39
Size (cm)	170	165			160	160	170	165	180
Weight (kg)	80	65			55	46	110	61	70
Delay (days)	6	8	7	6	9	4	7	4	11

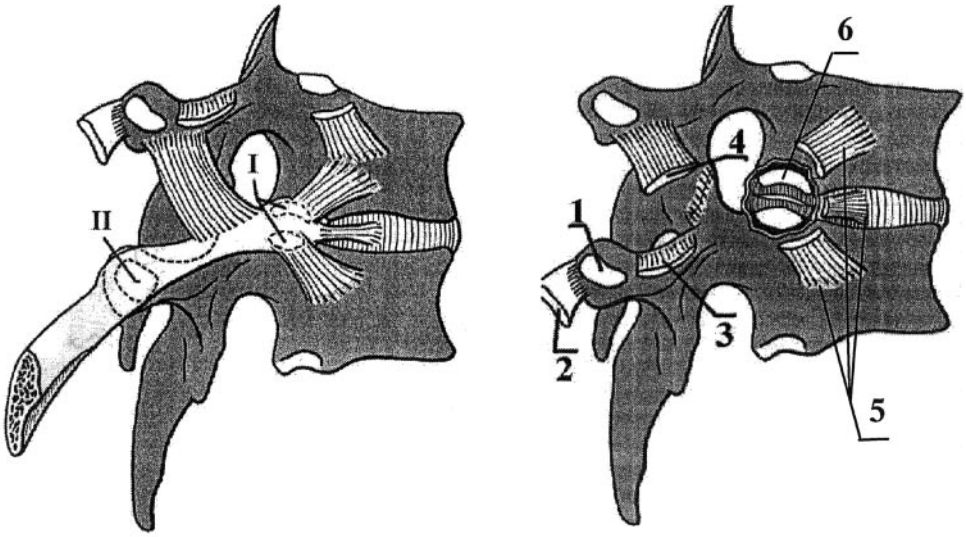

Fig. 1 Anatomy of the costo-vertebral and cost-transverse joints. *I* articulatio capitis costae, *II* articulatio costotransversaria, *1* fovea costalis transversalis, *2* ligamentum costotransversarium laterale, *3* ligamentum costotransversarium, *4* ligamentum costotransversarium superius, *5* ligamentum capitis costae radium, *6* ligamentum capitis costae intraarticulare

(Table 1). The anatomical samples were sterilized by β irradiation (2.5 Mrads) and kept frozen at –30° C until use.

One functional unit consists of two consecutive thoracic vertebrae (T), and the corresponding ribs (R), on each side of the spine. For each thoracic cage, we studied three levels. T1-T2-R2, T5-T6-R6, T9-T10-R10. We kept only the first 12 cm of the ribs.

There are two joints between the spine and a rib (Fig. 1): the costo-vertebral (articulatio capitis costae) and the costo-transverse (articulatio costotransversaria).

The costo-vertebral joint is a double arthrodial joint between the rib head on the one hand and the two consecutive vertebral bodies (foveae costales) and the discus intervertebralis on the other hand. The capsule is reinforced by the intra-articular costal head ligament and the anterior and posterior costo-vertebral ligaments. The costo-transverse joint is a simple arthrodial joint between the dorsal part of the tuberculum costae (facies articularis tuberculi costae) and the ventral plane of the processus transversus (fovea costalis transversalis). The capsule is reinforced by the lateral (ligamentum costotransversarium laterale), superior (ligamentum costotransversarium superius) and interosseous (ligamentum costotransversarium) costo-transverse ligaments.

We defined a joint local coordinate system (Fig. 2) for loading and measurements. The centre of this coordinate system was the centre of the costo-vertebral joint. The *X* axis was the rib cervical axis, which is the preferential axis of the costo-vertebral joint motion. The *Y* axis was the normal vector from the articular facet of the transverse process, and the *Z* axis was perpendicular to the first two.

Experimental set-up

The loading system

A metal rod passing through the medullar canal was used to fix rigidly the functional unit to the testing frame (Fig. 3). A pinch was attached to the rib without using glue or cement, to avoid risks of bony fracture (Fig. 4). A loading disc was fixed to this pinch with

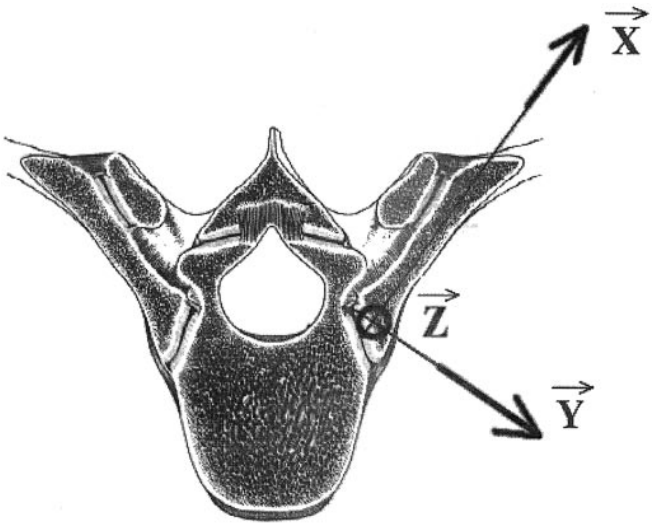

Fig. 2 Local coordinate system: *X* rib neck axis, *Y* normal to the costotransverse facet

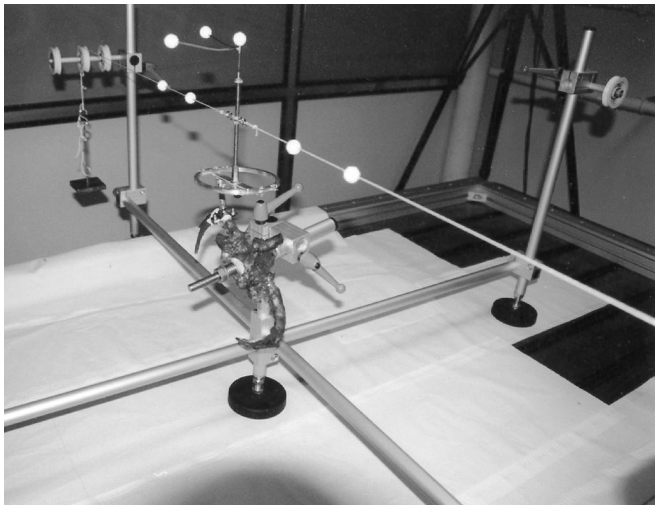

Fig. 3 Global view of the experimental set-up

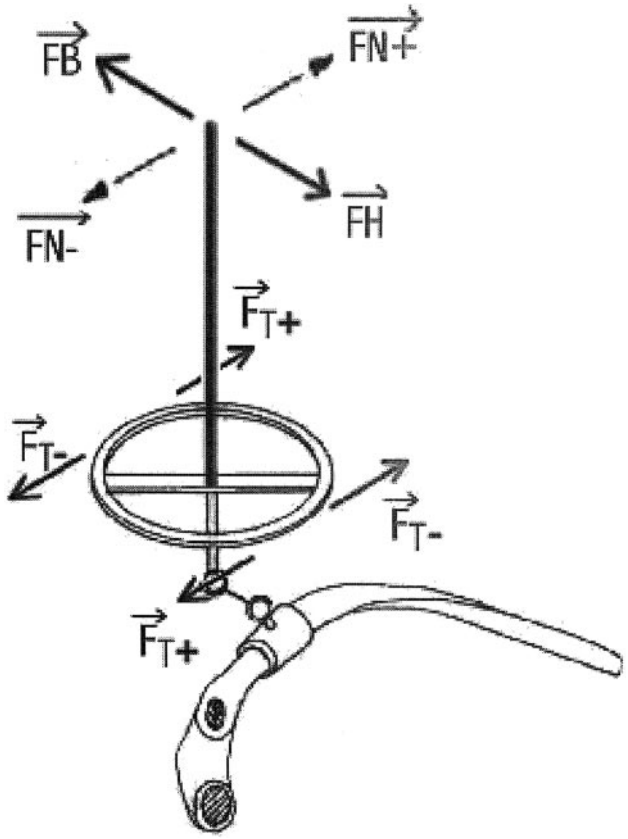

Fig. 4 Loading system with the different loadings. (F_{T+} cranial torsion, F_{T-} caudal torsion, F_{N+} ventral flexion, F_{N-} dorsal flexion, F_H cranial flexion, F_B caudal flexion)

a couple of ball-and-socket joints in such a way as to place the disc perpendicular to the local *X* axis. The loading system total weight was only 109 g. It was necessary not to use a heavy loading system to study such a low-stiffness joint.

A mass-and-pulley system was used. The threads winding round the disc applied a torque in the rib cervical axis (torsion around the *X* axis). The disc diameter was about 10 cm and a 220-g mass was used for each loading step.

To obtain the ventral-dorsal and cranial-caudal flexion, we applied moments along the *Z* axis and the *Y* axis, using threads attached on a rod at 17.5 cm from the centre of the costo-vertebral joint and we used 56-g masses.

The motions measurement system

An opto-electronic system (Vicon 370; Oxford Electronics) using three infrared cameras allowed us to capture the 3D motions of reflecting markers (Fig. 3). Three of them formed a tripod attached to the rib via the loading system and were used to view its motions (Fig. 5). The others were placed on the threads to mark the direction of the loads. The markers' position in the global (calibration) coordinate system was recognized by the DLT (direct linear transformation) method. The accuracy of the Vicon system in our experimental conditions was about +/– 0.5°.

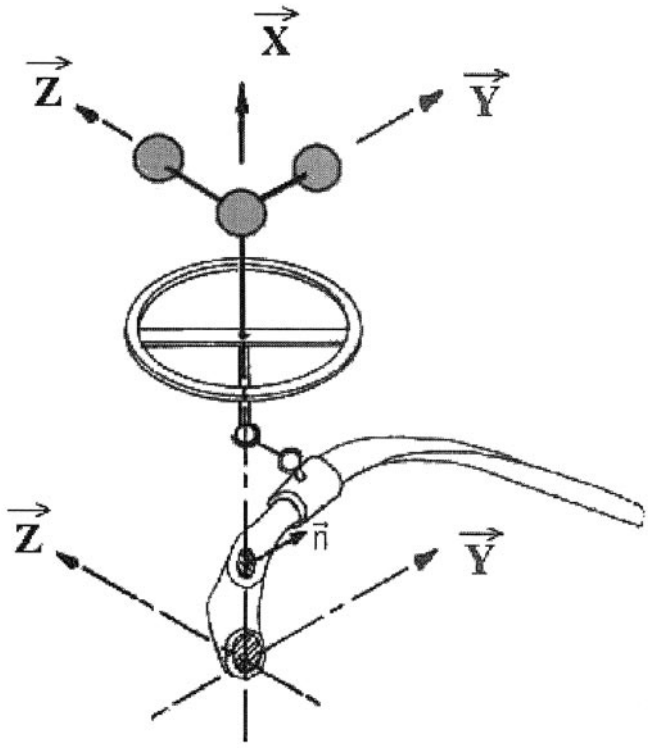

Fig. 5 The tripod formed by reflecting markers and its fixation onto the rib according to the local axes system

Procedure

Section of the ligaments

The functional unit was first tested intact, then after successive lesions of the superior, then the lateral and then the interosseous costo-transverse ligaments. Such tests allowed us to appreciate the role of the respective ligaments in the joint behaviour. Ease of anatomical access dictated the sequence of sections. Moreover, it was necessary that the joint motion was not excessively disturbed by the successive lesions. After interosseous ligament section, the behaviour was so much disturbed that the results were no longer consistent.

Loading cycle

The following loading cycle allowed us to observe the hysteresis and the different mechanical responses according to positive and negative loading directions. It started from +0.6 Nm, decreased step by step to –0.6 Nm (increment: 0.1 Nm), and finally increased back to +0.6 Nm.

Rotations calculation

The tripod position was recorded with the opto-electronic system at every loading step. Its initial position at zero load was used to determine the axes of the local coordinate system, and we calculated the angular motions of the joint in this coordinate system, using a fixed axes sequence *X*, *Y*, *Z*. Thus, we obtained load/displacement curves.

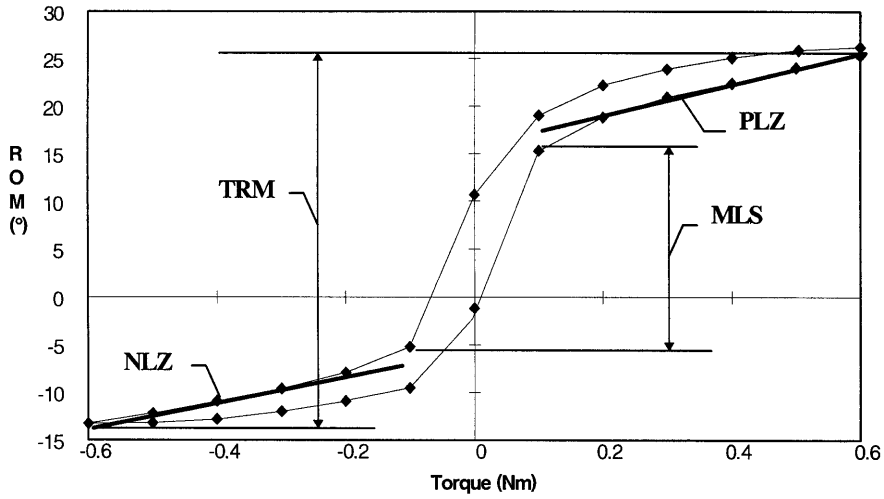

Fig. 6 Parameters defined on load/displacement curves. (*TRM* total range of motion, *MLS* range of motion in the low-stiffness zone, *PLZ* slope in the positive linear zone, *NLZ* slope in the negative linear zone)

Curves analysis

The load/displacement curves show a primary rotation in the loading direction and co-rotations (coupling motions) along the other axes. These co-rotations presented great variations, which were difficult to explain. We decided to analyse mainly the primary rotation at first. Four mechanical parameters were sufficient to describe every load/displacement curve in the primary rotation (Fig. 6):

The total range of motion between –0.6 Nm and +0.6 Nm (TRM)
The range of motion in the low-stiffness zone (MLS) between –0.1 Nm and +0.1 Nm
The slope in the positive linear zone (PLZ)
The slope in the negative linear zone (NLZ)

These slopes, characterizing the flexibility of the junction in the relevant direction, were defined from the regression line in the quasi-linear zone between 0.2 Nm and 0.6 Nm. (–0.2 Nm and –0.6 Nm).

Results

The mean value and the standard deviation of the mechanical parameters and the number of tested ribs for each case are shown in Tables 2, 3 and 4.

Torsion (Table 2)

The positive direction was the cranial torsion, and the negative one the caudal torsion.

From Table 2 it is obvious that the T1-T2-R2 level appeared to have the greatest total range of motion (TRM): 40.6° for intact units. The TRM at T9-T10-R10 (28.4°) was slightly greater than that at T5-T6-R6 (21.8°). This was due to the range of motion in the low-stiffness zone (MLS): 13.2° versus 8.1°. The radius of the sixth costal arc is one of the greatest in the complete thorax. This could explain why a smaller costo-vertebral movement is necessary to expand the thorax at this level.

The slopes in the positive linear zone (PLZ) and negative linear zone (NLZ), representing flexibilities, had the same grading as TRM. After the successive lesions we considered the flexibility to have changed significantly if it had increased by more than 5%.

The superior costo-transverse ligament (SCTL) section does not modify the T5-T6 flexibility of 12.7°/Nm in caudal torsion. Neither the SCTL section nor the lateral costo-transverse ligament (LCTL) alters the T9-T10-R10 flexibility in cranial torsion (11.1° then 11.3° then 11.3°/Nm) and in caudal torsion (14.4° then 14.2° then 14.5°/Nm). The whole stiffness seems to be maintained by the costo-vertebral part alone. This level is near the lower thoracic levels, where the costo-transverse part of the joint does not exist.

Finally, the interosseous costo-transverse ligament (ICTL) section alters very significantly the T1-T2 flexibility in caudal torsion (23.6° then 50.3°/Nm) but not in cranial torsion (20.4° then 19.3°/Nm).

Cranial and caudal flexion (Table 3)

The positive direction of loading was the cranial flexion and the negative one was the caudal flexion.

Like in torsion, the intact T5-T6 level had the smallest TRM, at 9.7°. However, in this case, the T9-T10 level had an even larger TRM than the T1-T2 level: 18.1° versus 13.7°.

The MLSs were very small at the T1-T2 and T5-T6 levels: 2.7° and 2.3° respectively. The T9-T10 level MLS amounted to 9.3°. The flexibilities of the different intact levels appeared to be similar, 6.2° and 6.1°/Nm for T1-T2 and T5-T6 levels in cranial flexion, and between 7.2° and 7.9°/Nm in caudal flexion. The successive sections made the flexibilities increase progressively except the SCTL section in cranial flexion at the T1-T2 level (6.2° then 6.2°/Nm) and in caudal flexion at the T9-T10 level (7.9°

Table 2 Mean and standard deviation values of the parameters with a torsion loading, for successive lesions of costotransverse ligaments: 0 = intact; 1 = superior; 2 = lateral; 3 = interosseous. *TRM* total range of motion (degrees), *MLS* range of motion in the low-stiffness zone (degrees), *PLZ* flexibility in the positive linear zone (degrees/Nm), *NLZ* flexibility in the negative linear zone (degrees/Nm), *n* number of tested junctions

		Level T1-T2								
		TRM		MLS		PLZ		NLZ		*n*
		Average	SD	Average	SD	Average	SD	Average	SD	
Lesion	0	40.6	7.4	21.1	6.4	16.3	2.4	15.3	2.1	11
	1	42.4	6.6	22.3	6.2	17.3	5.0	17.1	5.0	14
	2	48.0	4.9	24.2	3.6	20.4	8.8	23.6	5.9	12
	3	67.2	13.2	28.9	9.1	19.3	8.1	50.3	42.6	6
		Level T5-T6								
		TRM		MLS		PLZ		NLZ		*n*
		Average	SD	Average	SD	Average	SD	Average	SD	
Lesion	0	21.8	3.7	8.1	2.0	9.9	2.3	12.7	3.5	12
	1	22.4	4.0	8.6	2.4	10.5	2.1	12.7	3.5	11
	2	24.6	5.2	9.4	2.4	11.2	2.7	14.4	5.8	12
	3	29.7	6.0	14.6	5.3	12.6	2.6	14.9	4.8	10
		LEVEL T9-T10								
		TRM		MLS		PLZ		NLZ		*n*
		Average	SD	Average	SD	Average	SD	Average	SD	
Lesion	0	28.4	5.8	13.2	6.4	11.1	3.6	14.4	5.1	13
	1	29.5	6.6	14.5	6.6	11.3	3.2	14.2	2.9	14
	2	32.2	7.1	16.2	6.8	11.3	3.1	14.5	3.3	14
	3	37.8	8.9	19.7	8.6	13.0	3.7	16.0	5.4	12

Table 3 Mean and standard deviation values of the parameters with a cranial/caudal flexion loading

		Level T1-T2								
		TRM		MLS		PLZ		NLZ		*n*
		Average	SD	Average	SD	Average	SD	Average	SD	
Lesion	0	13.7	4.6	2.7	2.1	6.2	1.8	7.8	2.1	12
	1	13.3	4.9	3.1	2.0	6.2	1.6	8.6	3.0	12
	2	21.0	9.6	7.1	4.1	6.7	1.0	11.3	4.8	11
	3	39.6	10.2	22.6	7.2	10.9	3.3	16.8	5.6	3
		Level T5-T6								
		TRM		MLS		PLZ		NLZ		*n*
		Average	SD	Average	SD	Average	SD	Average	SD	
Lesion	0	9.7	2.3	2.3	0.8	6.1	2.0	7.2	2.8	13
	1	11.0	3.2	2.3	0.9	6.8	2.1	7.8	2.6	13
	2	12.9	3.4	3.4	1.4	7.1	2.0	9.5	3.7	14
	3	18.5	3.7	8.0	2.8	7.1	1.7	11.5	3.7	9
		LEVEL T9-T10								
		TRM		MLS		PLZ		NLZ		*n*
		Average	SD	Average	SD	Average	SD	Average	SD	
Lesion	0	18.1	7.1	9.3	5.2	7.3	3.1	7.9	3.5	13
	1	19.9	8.7	9.6	6.9	7.9	3.4	8.0	3.1	13
	2	22.9	9.1	11.9	7.7	8.4	2.7	8.9	5.1	14
	3	30.8	11.0	17.5	8.1	9.5	3.3	10.8	9.3	11

Table 4 Mean and standard deviation values of the parameters with a ventral/dorsal flexion loading

		Level T1-T2								
		TRM		MLS		PLZ		NLZ		*n*
		Average	SD	Average	SD	Average	SD	Average	SD	
Lesion	0	8.6	2.5	1.4	1.1	5.3	1.4	6.4	2.0	11
	1	9.5	2.7	1.9	1.6	6.2	0.9	6.7	1.5	11
	2	13.6	3.0	4.5	2.5	8.0	1.9	7.0	2.2	10
	3	47.1	12.4	28.6	8.5	31.6	19.9	7.6	1.0	4
		Level T5-T6								
		TRM		MLS		PLZ		NLZ		*n*
		Average	SD	Average	SD	Average	SD	Average	SD	
Lesion	0	6.1	1.2	0.7	0.5	5.5	1.8	5.0	1.5	13
	1	6.7	1.9	0.8	0.2	5.8	1.9	5.9	2.4	13
	2	8.5	2.4	1.4	0.4	6.7	2.1	6.1	2.2	14
	3	22.6	11.3	12.0	8.3	9.2	2.1	6.6	4.1	7
		LEVEL T9-T10								
		TRM		MLS		PLZ		NLZ		*n*
		Average	SD	Average	SD	Average	SD	Average	SD	
Lesion	0	16.2	3.7	6.2	3.4	7.3	3.7	7.2	3.1	13
	1	16.5	4.7	6.4	4.1	7.7	2.3	7.8	3.5	14
	2	18.9	4.9	8.4	4.4	9.4	3.5	7.9	3.3	14
	3	27.2	6.0	14.0	4.1	12.0	7.2	9.9	6.2	10

then 8.0°/Nm). The distal insertion of this ligament may be closer to the costo-transverse part of the joint at the T1-T2 level, decreasing its stress in cranial flexion. Conversely, the distal insertion was closer to the costo-vertebral part of the joint at the T9-T10 level, minimizing the role of this ligament in caudal flexion. Finally the ICTL section did not alter the T5-T6 level flexibility of 7.1°/Nm in cranial flexion.

Normal flexion (dorsal/ventral) (Table 4)

The positive direction of loading was the ventral flexion, and the negative one the dorsal flexion.

The T5-T6 and T1-T2 levels were not very flexible, with TRMs of 6.1° and 8.6°. The ranges of motion in the low-stiffness zone at these levels were very small: 0.7° and 1.4°. The flexibilities in the linear zone were similar, between 5.0° and 5.3°, except in the negative direction at T1-T2 level where it was 6.4°.

AS far as such a small range of motion can be analysed, the successive sections showed that the SCTL did not have a significant role in ventral flexion either at level T5-T6 (5.5° then 5.8°/Nm) or at level T9-T10 (7.3° then 7.7°/Nm).

As expected, the LCTL section did not significantly alter the dorsal flexion at any level. Finally the ICTL section made the T1-T2 joints so disturbed that their behaviour was no longer consistent.

Discussion

It was difficult to compare our methodology and results with those of other authors, because few data were available. Nevertheless, we did our best to examine critically our methods in order to produce valid results.

Criticisms about materials

The opto-electronic non-contact measurement system, avoiding friction, was very useful in following the 3D motion of this very low-stiffness joint.

Nine thoracic cages were involved. This is few considering the extent of anatomical disparities. However, the workload involved in studying each functional unit was very heavy. Our results certainly need confirming by other studies, but they still provide an initial database useful for modeling human spine.

The average age of the specimens was relatively high (61 years). However, all samples were free of any evident arthrosis or osteoporosis. No direct correlation was found between age and range of motion.

Out of each thoracic cage we selected only three anatomical levels to be tested. They were chosen in order to provide information on the superior, medium and inferior thoracic spine. Eleventh and 12th ribs are known to have unique characteristics, so we decided not to use them. The lowest common level is definitely the ninth rib level and the upper one is the second rib level, the medium level was chosen as the level halfway between these two. Unfortunately, these three levels presented such different mechanical behaviour that extrapolation for the intermediate levels would be uncertain. This problem became clear to us after the first results were examined. It was reasonable to assume that these differences were due to the morphology. We then decided to carry out semi-quantitative measurements in the next samples of our series. We do not yet know the importance of each morphological parameter.

Procedure criticisms

Because of its size, there was no means to attach the tripod close to the costal head and to make it visible to each camera. We therefore had to link it to the loading system fixed at 8 cm from the rib head. We then measured both the rib displacements and distortions, and the loading system distortion at the same time. These distortions could disturb the recording of the motion. According to another study carried out previously [6], the rib distortions in functional units this short can be considered as negligible compared with the joint motion.

Loads were applied according to the joint local coordinate system. Cranial and caudal torsions were the main clinically relevant loads since they produce the natural motion of the rib around its neck axis (the same motion occurs during breathing). The two other loading situations (normal and cranio-caudal flexions) were less clinically relevant, but are very useful in providing basic information, especially for finite-element modeling.

The quality of the trial depended on accurate positioning of the loading disc and the marker tripod according to the local coordinate system. Indeed, the local axes were defined using the marker tripod initial position (at zero load) and the loads were assumed to be applied along these local axes. Therefore, a small mistake in the positioning of the loading system provided a non-negligible error in measurements.

This positioning operation was carried out with great care and required a lot of time. The procedure had to be repeated as few times as possible during experiments, to avoid risks of error.

We tried to assess the repeatability error due to the loading system, the recording system, the time taken to carry out the experiment (and anatomical piece desiccation), etc. We repeated the same trial with the same anatomical piece, in the same circumstances. The differences were never more than 5%.

Results criticisms

Until the morphometric analysis we started is finished, we cannot explain the whole costo-vertebral behaviour from a physiological point of view. We can merely offer a few comments.

Observation of the range of motion shows that the T5-T6-R6 level is the most stiff, whatever the direction of loading. Probably, the radius of that rib (one of the largest) allows a wide linear displacement with a small angular rotation.

A systematic grading of each level and each load direction appeared to us the best way to analyse mechanical parameters. Finally, there was the relative problem of co-rotations along the other local axes accompanying the primary rotation, especially during ventro-dorsal flexion (*Z* axis rotation).

We did not represent these co-rotations in summary Tables because they were not consistent and we could not separate the influence of manipulation errors from real co-rotations. We assumed that dorsal flexion stretched the costo-vertebral part of the joint and compressed the costo-transverse part; conversely, ventral flexion compressed the costo-vertebral part and stretched the costo-transverse part. An asymmetric stretch in anterior costo-vertebral ligaments during dorsal flexion may procure axial rotation (along the *X* axis). Furthermore, the transverse process deflected the rib neck up or down and led to a *Y* axis rotation.

The only experimental study available in the literature regarding isolated costo-vertebral joints is by Schultz et al. [9]. Unfortunately, the methodology they used was slightly different from ours. They applied forces according to a global coordinate system and measured the linear deflections of the ribs, while we applied moments and measured angular motions of the ribs according to a local coordinate system.

Even if the ranges of motion were not comparable, our results and theirs are in accordance concerning the high flexibility of this joint, its non-linear behaviour and the existence of coupling motions.

Conclusions

The purpose of this study was to provide quantitative information, non-existent so far, about the mechanical behaviour of the costo-vertebral joint: ranges of motion, flexibilities in different loading directions and influence of the section of different ligaments on these parameters.

We are not yet able to explain exactly the whole joint mechanical behaviour, especially the co-rotations and the non-negligible difference in behaviour from one level to another. Morphometric analysis and modeling of the costo-vertebral joint and of the whole human spine are in progress, and this is expected to yield further explanations.

References

1. Andriacchi T, Schultz AB, Belytschko T, Galante J (1974) A model for studies of mechanical interactions between the human spine and rib cage. J Biomech 7:497–507
2. Aubin CE, Dansereau J, Labelle H (1992) Incorporation of costo-vertebral joints modelisation into a personalized finite element model of the scoliotic spine: application for simulation of Boston brace correction. International Symposium on 3D Scoliotic Deformities. Editions polytechnique de Montreal, pp 400–407
3. Aubin CE, Saint-Cyr E, Skalli W, Diop A, Kieffer G, Dansereau J (1995) Mechanical characterization and modelling of human costo-vertebral and costo-transverse articulations. In: D'Amico M et al. (eds) Three dimensional analysis of spinal deformities. IOS Press, Italy, pp 139–143
4. Closkey RF, Schultz AB, Luchies CW (1992) A model for studies of the deformable rib cage. J Biomech 25: 529–539
5. Jiang H, Raso JV, Moreau MJ, Russell G, Hill DL, Bagnall KM (1994) Quantitative morphology of the lateral ligaments of the spine. Spine 19:2676–2682
6. Maltais C (1994) Caractérisation et modélisation des articulations costo-vertébrales et costo-transversaires. Mémoire de Fin d'Etude, Ecole Polytechnique de Montreal and Laboratoire de Biomécanique de l'ENSAM, Paris
7. Marec P (1995) Analyse du comportement biomécanique de la jonction costo-vertébrale. Mémoire de DEA. Laboratoire de Biomécanique de l'ENSAM, Paris
8. Minotti P, Lexcellent P (1994) Geometric and kinematic modeling of a human costal slice. J Biomech 24:213–221
9. Schultz AB, Benson DR, Hirsch C (1974) Force deformation properties of human costo-vertebral articulations. J Biomech 7:311–318
10. Stokes IAF (1994) Three-dimensional terminology of spinal deformity. Spine 19:236–248
11. White III AA, Panjabi MM (1990) Physical properties and functional biomechanics of the spine. The rib cage. In: White III A et al (eds) Clinical biomechanics of the spine. Lippincott, Philadelphia, pp 55–59